Research Paper

PAIN

OPEN

Active role of the central amygdala in widespread mechanical sensitization in rats with facial inflammatory pain

Mariko Sugimoto[a,b], Yukari Takahashi[a], Yae K. Sugimura[a], Ryota Tokunaga[a], Manami Yajima[a,c], Fusao Kato[a,*]

Abstract

Widespread or ectopic sensitization is a hallmark symptom of chronic pain, characterized by aberrantly enhanced pain sensitivity in multiple body regions remote from the site of original injury or inflammation. The central mechanism underlying widespread sensitization remains unidentified. The central nucleus of the amygdala (also called the central amygdala, CeA) is well situated for this role because it receives nociceptive information from diverse body sites and modulates pain sensitivity in various body regions. In this study, we examined the role of the CeA in a novel model of ectopic sensitization of rats. Injection of formalin into the left upper lip resulted in latent bilateral sensitization in the hind paw lasting >13 days in male Wistar rats. Chemogenetic inhibition of gamma–aminobutyric acid-ergic neurons or blockade of calcitonin gene-related peptide receptors in the right CeA, but not in the left, significantly attenuated this sensitization. Furthermore, chemogenetic excitation of gamma-aminobutyric acid-ergic neurons in the right CeA induced de novo bilateral hind paw sensitization in the rats without inflammation. These results indicate that the CeA neuronal activity determines hind paw tactile sensitivity in rats with remote inflammatory pain. They also suggest that the hind paw sensitization used in a large number of preclinical studies might not be simply a sign of the pain at the site of injury but rather a representation of the augmented CeA activity resulting from inflammation/pain in any part of the body or from activities of other brain regions, which has an active role of promoting defensive/protective behaviors to avoid further bodily damage.

Keywords: Designer receptor exclusively activated by a designer drug, Clozapine-N-Oxide, VGAT-cre rat, Amygdala lateralization, Calcitonin gene–related peptide receptor, Adeno-associated virus, GABAergic neurons, von Frey filament test, Mechanical allodynia, Central sensitization, Latent orofacial formalin model, Latent inflammatory pain

1. Introduction

Widespread or ectopic sensitization is a hallmark symptom of chronic pain, characterized by aberrantly enhanced pain sensitivity in multiple body regions remote from the original tissue damage. For example, patients with temporomandibular disorders exhibit higher sensitivity to tourniquet, pressure, and heat pain at extracranial body sites, such as the forearm, hand, anterior tibialis, and epicondyle.[16,31,73] Patients with migraine often show cutaneous allodynia in widespread body regions, such as the forearm and face.[7,10,65] Likewise, in various preclinical models, aberrantly elevated sensitivity to touch or thermal stimulation at a body site distinct from the experimental injury or inflammation has been widely documented. For example, intraplantar injection of formalin in unilateral hind paw of rats and mice results in long-lasting mechanical and heat hyperalgesia at the dorsum of the injected foot and contralateral noninjected hind paw.[4,25,51,75] Reportedly, formalin injection in the tail facilitates the withdrawal response of the hind paw to heat stimulation,[8,9] and infraorbital nerve injury in rodents results in tactile allodynia and thermal hyperalgesia in bilateral hind paws.[81,88] Various models of migraine in rodents have shown potent mechanical sensitization not only in the face/head but also in the hind paw.[11,13,49] Although the mechanisms underlying these human and experimental animal cases of ectopic and widespread pain sensitization remain poorly explored, plastic changes and aberrant activity in the brain network involved in nociceptive signal processing and control of descending pain modulation may underlie these reported cases of widespread sensitization.

The central amygdala (CeA) is a kernel site for the nociceptive signal processing and control of descending pain modulation. The nociceptive signals from various regions of the body conveyed by the trigeminal and spinal nerves converge at the CeA[1,2,69,80] by the lateral parabrachial nucleus (LPB).[45,59] Unilateral orofacial inflammation increases the number of c-Fos-expressing neurons and potentiates LPB-CeA synaptic

Sponsorships or competing interests that may be relevant to content are disclosed at the end of this article.

[a] Center for Neuroscience of Pain and Department of Neuroscience, The Jikei University School of Medicine, Tokyo, Japan, [b] Department of Anesthesiology, Teikyo University School of Medicine, Tokyo, Japan, [c] Department of Dental Anesthesiology, School of Dental Medicine, Tsurumi University, Yokohama, Japan

**Corresponding author. Address: Department of Neuroscience, The Jikei University School of Medicine, 3-25-8 Nishishimbashi, Minato-ku, Tokyo 105-8461, Japan. Tel.: +81 3 3433 1111; fax: +81 3 5400 1231. E-mail address: fusao@jikei.ac.jp (F. Kato).*

Supplemental digital content is available for this article. Direct URL citations appear in the printed text and are provided in the HTML and PDF versions of this article on the journal's Web site (www.painjournalonline.com).

PAIN 00 (2021) 1–14

http://dx.doi.org/10.1097/j.pain.0000000000002224

transmission predominantly in the right CeA.[56] Recent studies show chemogenetic, optogenetic, and pharmacological modulation of the excitability of the CeA neurons, particularly those on the right side, alters the nociceptive sensitivity.[72,85] This suggests that the CeA regulates the nociceptive sensitivity in widespread regions of the body through divergent descending projections. These pieces of evidence suggest that peripheral inflammatory pain activates the CeA neurons, which in turn modulates sensitivity to nociceptive inputs. In this study, we demonstrate that chemogenetic inhibition of the gamma-aminobutyric acid (GABA)-ergic neurons in the right CeA, but not those in the left CeA, and also blockade of receptors for calcitonin gene–related peptide (CGRP), a neuropeptide involved in LPB-to-CeA neuromodulation,[18,46] in the right CeA, attenuates the latent ectopic mechanical allodynia occurring in the hind paw of a rat with facial inflammation. In addition, we demonstrate that chemogenetic excitation of the GABAergic neurons in the right CeA induces de novo mechanical sensitization in the bilateral hind limbs of a naïve rat. These results indicate that the right CeA is the kernel site for ectopic/widespread sensitization both in the presence and absence of primary causes, including tissue damage, inflammation, and noxious stimulation.

2. Materials and methods

2.1. Ethical statement

The manipulation of rats was in accordance with the Guidelines for the Proper Conduct of Animal Experiments of the Science Council of Japan (2006) and was in accordance with International Association of the Study of Pain guidelines. All the experiments were approved by the Institutional Animal Care and Use Committee of Jikei University (2015-008; 2016-066).

2.2. Animals

The animals in all experiments were always housed in individually ventilated cages with 2 to 3 rats/cage, with free access to food and water and placed in a temperature/humidity-controlled room with a light/dark cycle (7:00-19:00, white light; 19:00-7:00, red light). The floor of this home cage was covered with conventional soft animal floor bedding (Alpha-dri, EP Trading, Tokyo, Japan). The following 2 strains of rats were used: (1) Wistar/ST rats (Slc: Wistar/ST; Japan SLC, Inc, Shizuoka, Japan; referred to as Wistar rats hereafter) and (2) vesicular GABA transporter-cre BAC transgenic rats (referred to as VGAT-cre rats hereafter). The VGAT-cre rats were developed by the authors[36] and deposited to the National BioResource Project—Rat, Kyoto University (Kyoto, Japan; Rat ID, No.0839; W-Tg(Slc321-cre)$^{3\_5Fusa}$. VGAT-cre rats were of Wistar strain origin (Crlj:WI; Charles River Laboratories Japan, Inc) and were bred and raised in the Laboratory Animal Facility of Jikei University under the same conditions as described above. Information as to genotyping methods is available on request to the National BioResource Project. Only male rats were used in this study to minimize the influence of hormonal variation.

2.3. Experimental protocols

The following 4 sets of experiments (experiments 1–4) were performed: (1) Experiment 1: effect of upper lip formalin injection on bilateral 50%-estimate of the paw withdrawal threshold (PWT50) in Wistar rats. (2) Experiment 2: effect of activating hM4Di receptors (an inhibitory Designer Receptor Exclusively Activated by a Designer Drug [DREADD]) in brain slices and in vivo in VGAT-cre rats. (3) Experiment 3: effect of activating hM3Dq receptors (an excitatory DREADD) in brain slices and in vivo in VGAT-cre rats. (4) Experiment 4: effect of intra-amygdala administration of CGRP receptor antagonist in Wistar rats. The Wistar rats weighed 200 to 300 g when they were transported to the Laboratory Animal Facility of the Jikei University and were raised in the same facility as described above until the use (weight, 400–500 g at the day of behavior observation; 277-289 g for the experiments with long-term (>3 weeks) observation). The details of each manipulation are described below.

2.4. Adeno-associated virus vector microinjection into the CeA of VGAT-cre rats

VGAT-cre rats (5-9-weeks old; 145-434 g at the day of microinjection) were used for cre recombinase-dependent expression of exogenous molecules in the CeA and subsequent DREADD activation experiments (experiment 2 and 3). Rats were anesthetized with isoflurane (1%-2% in 100% O_2), and their head was fixed to a stereotaxic frame (Narishige, Tokyo, Japan). Under topical infiltration of ropivacaine (0.75%, 0.3 mL; Anapeine, aspen JAPAN, Japan) into the scalp, an incision was made to expose the skull surface. A small hole was drilled in the skull, and the underlying dura was removed. Using a 2-μL Hamilton syringe with a 30-gauge needle (65459-01; Neuros Syringe; Hamilton Company, Reno, NV), 0.7 μL virus suspension containing an adeno-associated virus (AAV) (serotype 5) encoding one of the following 3 different constructs was delivered into bilateral or unilateral CeA: (1) AAV-hSyn-DIO-hM4Di-mCherry, (2) AAV-hSyn-DIO-hM3Dq-mCherry, and (3) AAV-hSyn-DIO-mCherry (UNC Gene Therapy Center Vector Core, Chapel Hill, NC). The injection was administered at a rate of 50 nL/min controlled with a microsyringe pump (UltraMicroPump II with SYS-Micro4 Controller, UMP2, UMC4, World Precision Instruments, Sarasota, FL). The injection syringes were allowed to remain in place for an additional 10 minutes to allow for virus diffusion before withdrawal.[74,79] The solution also contained 0.095% fluorescent microspheres (FluoSpheres; 0.02 μm, blue 365/415; Life Technologies, Waltham, MA) for postexperiment certification of the injection sites (see below). The stereotaxic coordinate for this injection was 1.9 to 2.3 mm caudal to the bregma, 3.8 to 4.2 mm lateral to the midline, and 7.5 to 8.2 mm ventral to the dorsal brain surface, which was empirically adjusted according to the size and age of the rat. For ex-vivo verification of the functional DREADD expression, 2 rats were injected with a 0.5-μL solution containing an AAV-hSyn-DIO-hM4Di-mCherry virus (experiment 2) into the right (n = 1) and left (n = 1) CeA, and 3 rats were injected with a 0.7-μL solution of AAV-hSyn-DIO-hM3Dq-mCherry virus (experiment 3) to the right (n = 2) or bilateral (n = 1) CeA, respectively. After completion of the injection procedure, the skin was sutured with 4-0 silk threads, and the rats were placed in their home cages. In these VGAT-cre rats, 1 week after the AAV vector microinjection, daily acclimation was started for 2 weeks, and formalin or saline was administered to the upper lip 3 weeks after the microinjection.

2.5. Implantation of guide cannula for intra-amygdalar application of calcitonin gene–related peptide receptor antagonist in Wistar rats

A week before the upper lip injection experiments, the brain of a Wistar rat was exposed in the same manner as with the AAV vector microinjection described above under isoflurane anesthesia. A stainless guide cannula (8-mm long, 26-gauge; Model

C315G, Plastics One, P1 Technologies, Roanoke, VA) was slowly implanted into either one of the right, left or bilateral CeA, using a micromanipulator (the coordinates were 2.2-2.4 mm caudal to the bregma, 4.1-4.2 mm lateral to the midline, and 7.0-7.5 mm below the brain surface) (experiment 4). For the placement control experiments, the guide cannula (5-mm long) was implanted into the bilateral striatum (2.2-2.6 mm caudal to the bregma, 4.6-4.8 mm lateral to the midline, and 4.3-4.5 mm below the brain surface). The guide cannula was fixed to the skull using dental acrylic cement covering 4 microscrews inserted into the skull. Stylets 8-mm (for the CeA-targeting cannulas) or 5-mm (for the striatum-targeting ones) in length were inserted into the guide cannula to prevent clogging until immediately before the drug application.[74] The rats were allowed to recover for 5 days in the home cage before recording the "baseline" PWT50 measurement (see below), which was made a day before the upper lip formalin injection.

2.6. Evaluation of PWT50 (von Frey test)

From 2 weeks before the day of the upper-lip formalin injection experiments, the rats were habituated in the allodynia observation chamber (25 cm × 25 cm, mesh floored) for 1 hour every day under red ambient illumination. The PWT50 of the bilateral hind paws was evaluated in the same chamber after acclimation for 30 minutes. A calibrated series of von Frey filaments (0.4 g–15 g; North Coast Medical, Inc, Gilroy, CA) was applied to the plantar aspect of the hind paws from underneath the mesh floor. The withdrawal response was judged by one of the experimenters without explicit knowledge of the animal number and treatment type, to evaluate the 50% response threshold with the up-and-down method.[19] The evaluators were blinded to the type of the injected AAV (experiment 2 and 3) and were semiblinded to the type of solution injected to the upper lip (see below for upper lip formalin injections) and presence of facial swelling by putting the chamber in a dark room with minimal light to observe the hind limb movement (in all von Frey filament tests). Because of this dark room and minimal light, the experimenter could not see the face of the rats. However, if one dared to see the face, one can guess whether the rat has swelling on the cheek under dim light, which we tried not to do so. This is why it is described that it was performed in a semiblinded manner.

For experiments 2, 3, and 4, the PWT50 measured 1 day before the formalin or saline injection was used as a "baseline" value. In experiment 1, in which only the formalin effect was observed, the PWT50 evaluated at 1 week before the injection was used as the "baseline" value. The details of the timing of PWT50 measurements are described in the schema in each figure describing the results.

2.7. Orofacial inflammatory pain and evaluation of acute nocifensive behaviors

In each experimental session, the rats were assigned to either formalin or saline injection group according to their "baseline" PWT50 values to equalize their means as much as possible. Otherwise, a random block design was applied. After acclimatization for ~30 minutes in an acrylic observation chamber (17 cm × 17 cm × 35 cm) with 3 mirrors to video-capture rat behaviors, 50 μL of 5% formalin solution (Nacalai Tesque Inc, Kyoto, Japan) or an equal volume of saline was injected into the left upper lip of the rat (the upper lip), just lateral to the nose, using a 0.3-mL syringe with a 30-gauge needle (Becton, Dickinson and Company, Franklin Lakes, NJ), and the acute nociceptive behaviors[20,21,68] of the rat were video-recorded with a PC for 60 minutes with a web camera (Logicool HD Webcam C525, Logicool Co, Tokyo, Japan). During injection, the rats were held softly with a towel, to which they were acclimatized every day for 1 to 2 weeks during the habituation period, which made anesthetics unnecessary. The duration of time spent in face rubbing behavior was measured postexperimentally by evaluation of the video playback by an evaluator blinded to the rat group. The observation chamber did not have food or water supply.

2.8. Ex-vivo verification of the designer receptor exclusively activated by a designer drug expression (experiments 2 and 3)

2.8.1. Slice preparation for electrophysiological recordings

At 5 to 8 weeks after virus injection, brain slices were prepared for electrophysiological recordings according to previously described procedures from our laboratory.[79] This timing was somewhat later than the behavioral tests, simply because of the availability of the rat for electrophysiology, and we did not find any difference in responses to clozapine N-oxide (CNO) reported below and fluorescence expression in the slices made at later stages. The rats were first perfused transcardially with an ice-cold cutting solution under isoflurane anesthesia (5% in 100% O_2), and the brain was removed. A block of the forebrain containing the amygdala was dissected out and cut at the midline in the ice-cold cutting solution composed of (in mM) 2.5 KCl, 0.5 $CaCl_2$, 10 $MgSO_4$, 1.25 NaH_2PO_4, 2 thiourea, 3 sodium pyruvate, 93 N-methyl-D-glucamine, 20 HEPES, 12 N-acetyl-L-cysteine, 25 D-glucose, 5 L-ascorbic acid, and 30 $NaHCO_3$ equilibrated with 95% O_2 + 5% CO_2 (osmolarity, approximately 290 mOsm/kg; pH of the solution was titrated to 7.1-7.5 with concentrated HCl). The dissected hemisphere containing the amygdala was secured on the cutting stage of a vibrating blade slicer (PRO 7; Dosaka EM, Kyoto, Japan) with the rostral end upward to cut coronal slices. The dissected hemisphere was immediately embedded in a 37°C agarose solution (1.6%; Sigma-Aldrich, Missouri, MO), which was solidified by immediate cooling by covering it with the ice-cold cutting solution, and brain slices of 300-μm thickness were prepared. The slices were first incubated in a holding chamber with a constant flow of cutting solution at 34°C for 15 minutes. After this initial recovery period, the slices were transferred to another holding chamber containing artificial cerebrospinal fluid (ACSF) composed of (in mM) 119 NaCl, 2.5 KCl, 2 $CaCl_2$, 2 $MgSO_4$, 1.25 NaH_2PO_4, 12.5 D-glucose, 5 L-ascorbic acid, 2 thiourea, 3 sodium pyruvate, and 26 $NaHCO_3$ (pH approximately 7.3, bubbled with 95% O_2 + 5% CO_2; osmolality, approximately 300-310 mOsm/kg H_2O) at room temperature (20-25°C) until electrophysiological recording. Each slice was transferred to a recording chamber (volume, approximately 0.4 mL) and fixed with nylon grids attached to a platinum frame. The slice was submerged in the chamber and superfused continuously at a rate of 1.8 to 3 mL/min with the ACSF described above.

2.8.2. Patch-clamp recordings in the CeA

Neurons in the CeA were identified visually under an upright microscope (BX-51WI; Olympus, Tokyo, Japan) with oblique illumination. Images from living slices during electrophysiological recordings were captured using a CCD camera (IR-1000; DAGE-MTI, Michigan City, IN) and stored digitally on a computer. Patch-clamp electrodes were made from borosilicate glass pipettes (1B120F-4; World Precision Instruments, Sarasota, FL). The tip

resistance of the electrode was 5 to 8 MΩ. The composition of the internal solution was (in mM) 120 potassium gluconate, 6 NaCl, 1 $CaCl_2$, 2 $MgCl_2$, 2 ATP Mg, 0.5 GTP Na, 12 phosphocreatine Na_2, 5 EGTA, and 10 HEPES hemisodium (pH 7.3 as adjusted with KOH; osmolarity, approximately 290 mOsm/kg). Whole-cell membrane potentials of transduced neurons (identified by mCherry fluorescence) were recorded using an Axopatch 700B amplifier (Molecular Devices, San Jose, CA), filtered at 2 kHz, and digitized at 10 kHz with 16-bit resolution using a PowerLab interface (AD Instruments, Dunedin, New Zealand). Input resistance, resting membrane potential, and whole-cell capacitance were measured immediately after the establishment of whole-cell mode by membrane rupture. The resting membrane potential was recorded (in current-clamp mode) in normal ACSF for 5 minutes before the addition of 5 μM CNO (Enzo Life Sciences Inc, Farmingdale, NY) for 3 minutes. Stock solutions of CNO were dissolved in water, kept frozen at −30°C, and then dissolved in ACSF to their final concentration on the day of the experiment. A rectangular hyperpolarizing pulse (100-300 ms, −20 pA) followed by a depolarizing pulse (500 ms, 100-120 pA) was injected every 10 seconds to observe electroresponsive properties of the neurons. All recordings were made at room temperature (20-25°C). Oblique illumination and epifluorescence images were captured using the same camera and were overlaid in Photoshop software (ver. 5.5; Adobe, San Jose, CA) with modification of the brightness and contrast alone.

2.9. In vivo clozapine N-oxide injection

Chemogenetic stimulation of the DREADD was conducted by intraperitoneal administration of CNO (3 mg/ml/kg), which was dissolved in normal saline immediately before administration, using 1 mL syringe and 27-gauge needle. The von Frey filament tests were repeated 15 minutes before and 45 minutes after each CNO administration considering the 30-min acclimation time to the test cage and reported time course of CNO effects in rodents.[33,70,71] Because of the possible off-target effects on endogenous receptors of CNO directly or after being metabolized to clozapine,[29] we did not compare CNO effects to those of vehicle in this study, but comparisons of the effect of DREADD activation were always made between rats with DREADD-expression and mCherry expression.[53] By doing so, we carefully avoided the influence of the effect of clozapine not mediated by DREADDs activation.

2.10. In vivo calcitonin gene–related peptide receptor antagonist injection into the CeA

Calcitonin gene–related peptide$_{8\text{-}37}$ *experiments (experiment 4)*. A CGRP1 receptor antagonist, calcitonin gene–related peptide fragment 8 to 37 (human $CGRP_{8\text{-}37}$, Phoenix Pharmaceuticals Inc, Burlingame, CA), was dissolved in normal saline at 1.8 μg/μL and frozen at −30°C until the day of infusion. Just before use, we added fluorescent microspheres (FluoSpheres; 0.02 μm, red 580/605; Life Technologies) to the solution at a concentration of 0.2%. A solution containing $CGRP_{8\text{-}37}$,[48,76,87] was infused through a 32-gauge injection cannula (Model C315I, Plastics One, P1 Technologies), with its tip extending beyond the end of the guide cannula (C315GA, Plastics One, P1 Technologies) by 2 mm. The other end was connected to a 10-μL microsyringe (Hamilton Company, Reno, NV) by a polyethylene tubing. On the drug infusion, a rat was gently held in the hand of a blinded experimenter without anesthesia, and the solution was injected at a rate of 0.25 μL/min using an infusion pump (KDS 200, KD Scientific, Holliston, MA) to achieve the final injected volume of 0.5 μL/side (900 ng/side). The injection cannula was left in place for an additional 2 minutes after injection of the 0.5-μL solution. The control solution did not contain $CGRP_{8\text{-}37}$.

2.11. Histological verification of the injection site, transfected molecule expression, and cannula placement

After the last behavioral experiment, the rats were given sodium pentobarbital (100 mg/kg, i.p.; Somnopentyl, Kyoritsuseiyaku Corporation, Tokyo, Japan) and immediately perfused intracardially with ice-cold 200 mL phosphate buffered saline (PBS) followed by 250 mL of 4% paraformaldehyde in 0.1 M phosphate buffer. The brains were removed and immersed in 20% (wt/vol) sucrose in PBS for 1 to 2 days. Then, they were frozen sectioned into 25-μm (experiments 2 and 3), or 50-μm (experiment 4) coronal slices using a cryostat (CM1850, Leica Biosystems, Tokyo, Japan), placed on slide glasses (Matsunami Glass Ind, Ltd, Osaka, Japan), every 200 μm (experiment 2, 3), or 50 μm (experiment 4), and coverslipped. In experiments 2 and 3, the fluorescence of mCherry and microspheres in the CeA were visualized by a fluorescence microscope (BX-63; Olympus, Tokyo, Japan). Somatic expression of mCherry fluorescence (for experiment 2) and fluorescence of FluoSphere (for experiment 3) were visually confirmed after registration of the slice to the Paxinos and Watson atlas[64] using PowerPoint, and the border of fluorescence signal was drawn on the atlas of corresponding brain levels.

2.12. Multiplex fluorescent in situ hybridization

To examine the expression of cre-recombinase with markers for glutamatergic and GABAergic neurons, we performed multiplex fluorescent in situ hybridization using RNAscope Fluorescent Multiplex Assay (Cat No. 320850, advanced cell diagnostics [ACD], Newark, CA; Medical and Biological Laboratory, Nagoya, Japan). Sections were processed according to the protocol provided by the manufacturer. In brief, the fresh frozen sections of 16-μm thickness were attached on glass slides, dried, and kept at −80°C until the day of in situ hybridization. On the day of reaction, the sections were fixed in ice-cold 10% normal buffered formalin for 15 minutes at 4°C. Then they were dehydrated for 5 minutes each at room temperature with increasing concentrations of ethanol (50%, 70%, and 100%) and were air dried. The sections were pretreated with double diluted protease III for 30 minutes at room temperature. After washing in PBS, the RNAscope probes, Rn-slc17a7 (317,001, ACD Inc.), Rn-slc32a1-C3 (424541-C3, ACD Inc.), and CRE-C2 (312281-C2, ACD Inc.), for detecting mRNAs for vesicular glutamate transporter 1 (VGLUT1), VGAT, Cre recombinase, respectively, and were applied on the sections and incubated for 120 minutes at 40°C. The signals were amplified using a hybridization oven according to the manufacturer's instructions. After the final wash, sections were stained with DAPI and mounted with Aqua-poly Mount medium (Polysciences, Warrington, PA) and were visualized with a confocal microscope (FV1200, Olympus, Tokyo, Japan) to visualize mRNA expression of VGAT, VGLUT1, and cre recombinase in the CeA.

2.13. Data and statistical analysis

The statistical comparisons were performed using SPSS 23 (IBM, Tokyo, Japan) or R with its interpreter EZR commander.[44] Values are expressed as the mean ± SEM. We made statistical comparisons according to the following principles. (1) Time-dependent changes in the values of the 2

groups. First, 2-way repeated-measures analysis of variance (ANOVA) using time and treatment (formalin and saline orofacial injections) was used to test if the values differ statistically depending on time and treatment and interaction between time and treatment. Then, post-hoc tests were performed to examine if the values differed statistically between treatments at each time point using Student's *t*-test in cases where the values at each point were governed by normal distribution or using the Mann–Whitney *U* test if the values do not follow a normal distribution. (2) Time-dependent changes in the values from more than 3 groups. First, 2-way repeated-measures ANOVA using time and treatment (formalin and saline orofacial injections in left and right paw measurements [ie, 4 groups]) was used to test if the values differ statistically depending on time and treatment and if there was an interaction between time and treatment. Then, post-hoc tests were performed using Gabriel Multiple Comparison test to examine whether the values significantly differ between groups at each time point and using Dunnett's test to examine if the values significantly varied from the baseline (ie, the values before treatment, the values after the initial treatment but before the following treatments, or both). (3) Comparisons between multiple groups with different treatments (formalin or saline for orofacial injection) and distinct DREADD vector (hM4Di, hM3Dq, and mCherry) injection into the CeA. First, we performed 2-way repeated-measures ANOVA to examine the effects of formalin injection and the effects of type of the DREADD vector and their interaction. Then we performed a post-hoc Gabriel test to examine if the values differ significantly between values of all combinations of formalin/saline and types of DREADD vectors at each time point. Finally, we used Dunnett's test to examine if the values significantly varied from the baseline in each treatment group (ie, the values before treatment (baseline) and the values before CNO administration were used as "control"). Only the results of scientifically meaningful comparisons are reported in the figures, but all possible comparisons were reported in Table 1 (available at http://links.lww.com/PAIN/B291). (4) Comparisons between multiple groups with different treatments (formalin or saline for orofacial injection) and distinct intracerebral injections of CGRP receptor antagonist or vehicle (vehicle or $CGRP_{8\text{-}37}$ into the CeA or $CGRP_{8\text{-}37}$ into the striatum). Comparisons were made in the same manners as in the case (3), but the post-hoc between-group comparisons at each time point were made with the Gabriel test (when there are more than 3 groups) or Mann–Whitney *U* test (for 2 groups), if any of the values did not satisfy the prerequisite of unpaired Student's *t*-test. (5) Comparisons of the values from the same neurons obtained before and after treatment (CNO application). We tested if the treatment significantly affected the values using the Student's paired *t* test. The results of the statistical tests were displayed in the figures, and the supplement table in detail (Table 1, available at http://links.lww.com/PAIN/B291). The necessary sample size for each comparison was estimated using the "sample mean" function of R with the previously obtained mean values and standard deviation with detection level at alpha = 0.01. This estimation gave approximately n = 9 for each group. The membrane potential and number of action potentials were measured and analyzed with Igor Pro 7 (WaveMetrics, Portland, OR) using procedures written by F.K. The details of the statistical tests are described in each figure legends. All graphs were made with Igor Pro 7. Differences with a probability (*P*) value smaller than 0.05 were considered significant.

3. Results

3.1. Mechanical hypersensitivity of the bilateral hind limb in the facial formalin model

In experiment 1, we first evaluated the baseline PWT50 with a von Frey filament test and, a week later, injected formalin solution to the subcutaneous tissue of the left upper lip (**Fig. 1A**). In agreement with already published studies using this orofacial formalin model,[56] the rats showed the "face rubbing" nocifensive behavior starting immediately after the injection, and this behavior lasted for ~45 minutes and faded away within 1 hour in all animals (**Fig. 1B**). The rats that received saline injection instead of formalin did not show such rubbing behavior (**Fig. 1B**).

It has been reported that an intraplantar formalin injection causes not only acute nocifensive behavior but also symptoms of long-lasting inflammation and neuropathic pain-like behavior starting at a few hours and lasting for a few weeks after the injection.[15,25–27,82,84,86] As this manifestation of latent symptoms could be considered to be a state comparable with the early stage of transition from acute to chronic pain, we examined if these rats showed a typical symptom of chronic pain, that is, ectopic sensitization.[11,62,88] In the rats with robust signs of rubbing behavior in the first 1 hour after upper lip formalin injection, we measured the PWT50 of the hind limb on both sides from 90 minutes postformalin injection up to 3 days (**Figs. 1A and C**). These formalin-injected rats showed a drastic and significant decrease in the PWT50 in bilateral hind limbs, which lasted up to our last measurement at 72 hours postinjection (**Fig. 1C**). Although there was a tendency of recovery in the right hind limb at 72 hours, the PWT50 was significantly lower than that at the baseline value, and that observed in the saline-injected rats (**Fig. 1C**) in both hind limbs at any time point of analysis (1.5-72 hours post-injection). This inflammation did not result in a significant time-dependent and a treatment-dependent difference in the body weight (Fig. S1, available at http://links.lww.com/PAIN/B292), suggesting that its influence on the feeding behaviors is, if any, limited at least within 3 days.

All rats receiving formalin injection showed reddish swelling around the site of formalin injection, but not on the other side, peaking at 25 hours and lasted till 73 hours after the injection (**Fig. 1D**), suggesting a sustained inflammation at the site of injection. This bilateral mechanical allodynia in the hind limb lasting for > 3 days after upper lip formalin injection was taken as a sign of ectopic sensitization appearing at a remote site from the primary inflammation. In another set of rats, we measured the PWT to 23 days after formalin injection and found a significant saline-to-formalin difference in either paw until 13 days postformalin (Fig. S2, available at http://links.lww.com/PAIN/B292), suggesting that this ectopic sensitization lasts long after the initial acute inflammatory responses.

3.2. Activation of inhibitory designer receptor exclusively activated by designer drugs in the CeA by clozapine N-oxide attenuates ectopic sensitization in the rats with orofacial inflammation and activation of excitatory ones induced mechanical hypersensitivity in noninflamed rats

It is highly likely that central mechanisms underlie this ectopic sensitization in the hind limb after orofacial inflammation. We have already demonstrated that the same manipulation of upper lip formalin injection results in robust synaptic potentiation and augmented c-Fos expression predominantly in the right CeA.[56] Based on this observation, we hypothesized that the increased

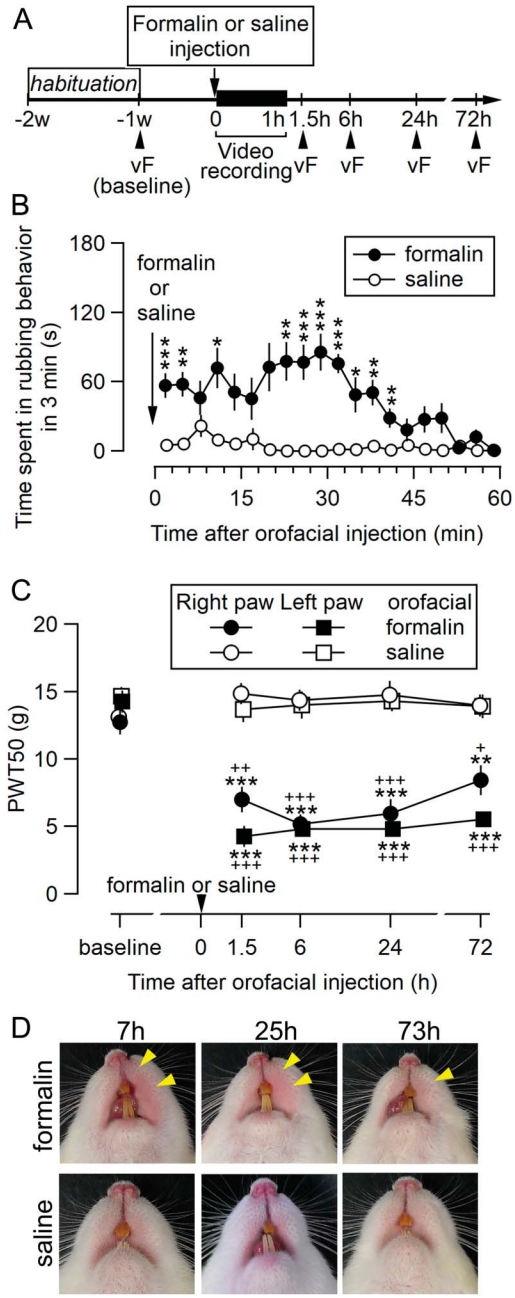

Figure 1. Nocifensive behaviors induced by formalin injection into the left upper lip. (A) Experimental procedure (experiment 1). "vF" with arrowheads, von Frey filament tests to hind paws. Video recording was performed for 60 minutes after upper lip formalin/saline injection in all behavioral experiments. (B) Summary of the time course of spontaneous nocifensive behavior (face rubbing) after an injection of 5% formalin (filled) or saline (open) to the left upper lip. The total time spent exhibiting nocifensive behavior within every 3-minute window is pooled. The markers placed in the middle of 2 x-axis ticks (eg, t = 0 and t = 3) represent the total sum within this 3-minute period. $^{*}P < 0.05$, $^{**}P < 0.01$, and $^{***}P < 0.001$ between formalin-injected and saline-injected groups; Mann–Whitney's *U* test; n = 8 per group (detailed statistical results are shown in Table 1, available at http://links.lww.com/PAIN/B291). (C) Mechanical PWT50 of the hind paws after upper lip injection of formalin/saline. $^{**}P < 0.01$, $^{***}P < 0.001$ between PWT50 of the right hind paw of formalin (filled circle)-injected and saline (open circle)-injected groups, or between PWT50 of the left hind paw of formalin (filled square)-injected and saline (open square)-injected groups; Gabriel's test. $^{+}P < 0.05$, $^{++}P < 0.01$, $^{+++}P < 0.001$, PWT50 of each hind paw after upper lip formalin injection compared with that of baseline; n = 8 per group (detailed statistical results are shown in Table 1, available at http://links.lww.com/PAIN/B291). (D) Typical example of swelling at the formalin/saline-injected site (left upper lip [right side of each photograph]). Yellow arrowheads indicate the area of swelling.

excitation of the CeA neurons might underlie this ectopic sensitization. To directly examine this, we used DREADD technology by prior transfection of AAV into the CeA of VGAT-cre rats, to limit the expression of DREADD molecules to the CeA neurons, most of which are GABAergic. First, we divided the VGAT-cre rats into 3 groups according to the type of AAV vector to be injected into the CeA: AAVs for the expression of hM4Di-mCherry, hM3Dq-mCherry, and mCherry alone. Next, the rats belonging to each of these 3 groups were randomly assigned to 3 subgroups: injection into the bilateral CeA, right CeA, and left CeA. Finally, the rats were further divided into 2 subgroups by the type of upper lip injection: formalin or saline. The experimental protocol and the timings of each manipulation are shown in **Figure 2A** together with the symbol color assignment for the type of AAV vectors transfected and type of drug injected to the upper lip (the box in the right of **Fig. 2A**). Here, we will describe the data for the formalin-injected group (**Fig. 2B**) and then those for the saline-injected group (**Fig. 2C**), the experiments for which were made in parallel. In describing the data from rats expressing inhibitory (hM4Di) or excitatory DREADDs (hM3Dq) in the CeA (represented with blue and orange circles, respectively, in **Fig. 2**), the data from rats receiving mCherry-expressing AAV (magenta circles) were used as the control group. These data are compared first using 2-way repeated ANOVA (time and groups) followed by post-hoc analyses with the Gabriel test for between-groups comparison and Dunnett's test for the testing changes from the baseline (−24 hours) and changes from the pre-CNO values (first and second administration) in each group.

The rats receiving formalin injection showed a robust and significant decrease in the PWT50 of both right and left hind paws, a clear sign of ectopic hypersensitivity (all filled circles at "5 hours" in **Fig. 2B**) at 5 hours after the injection. Intraperitoneal injection of CNO (3 mg/kg) administered at 5.25 hours after the formalin injection significantly increased this lowered PWT50 at 6 hours (ie, 45 minutes after the CNO administration) in the rats expressing hM4Di in the bilateral (blue-filled circles in **Fig. 2B1**) and right (**Fig. 2B2**) CeA, but not in those expressing hM4Di in the left CeA (blue-filled circles in **Fig. 2B3**). Clozapine N-oxide administered for the second time at 24.25 hours postformalin injection, at which the PWT50 had almost returned to the pre-CNO value measured at 5 hours, again resulted in a significant increase in the threshold of the bilateral hind paws at 25 hours in rats with hM4Di-expression in the bilateral or right CeA (blue-filled circles **Figs. 2B1 and B2**). Despite these significant increases in PWT50 by CNO from the value lowered by formalin injection at 5.25 hours and 24.25 hours postformalin in the rats expressing hM4Di, the PWT50 measured 45 minutes after CNO injection was still significantly smaller than the baseline value measured at 1 day before the formalin injection (Dunnett's test; **Figs. 2B1 and B2**), suggesting excitation of CeA neurons with CNO in the hM4Di-expressing rats increases PWT50 lowered by formalin, whereas this effect is not effective enough to recover the hypersensitivity completely. Again, CNO did not significantly affect the PWT50 of the rats with left CeA expression of hM4Di (**Fig. 2B3**). These CNO effects were not apparent or below the significance level in the rats injected with AAV for hM3Dq expression in formalin-treated rats (orange circles in **Fig. 2B**). These results indicate that selective suppression of right or bilateral CeA neuronal excitability attenuates ectopic mechanical allodynia. CNO injection to these rats with upper-lip formalin inflammation did not further decrease the PWT50 (**Figs. 2B1, B2, and B3**, filled orange circles), suggesting that the effect of exciting the CeA neurons, particularly those in the

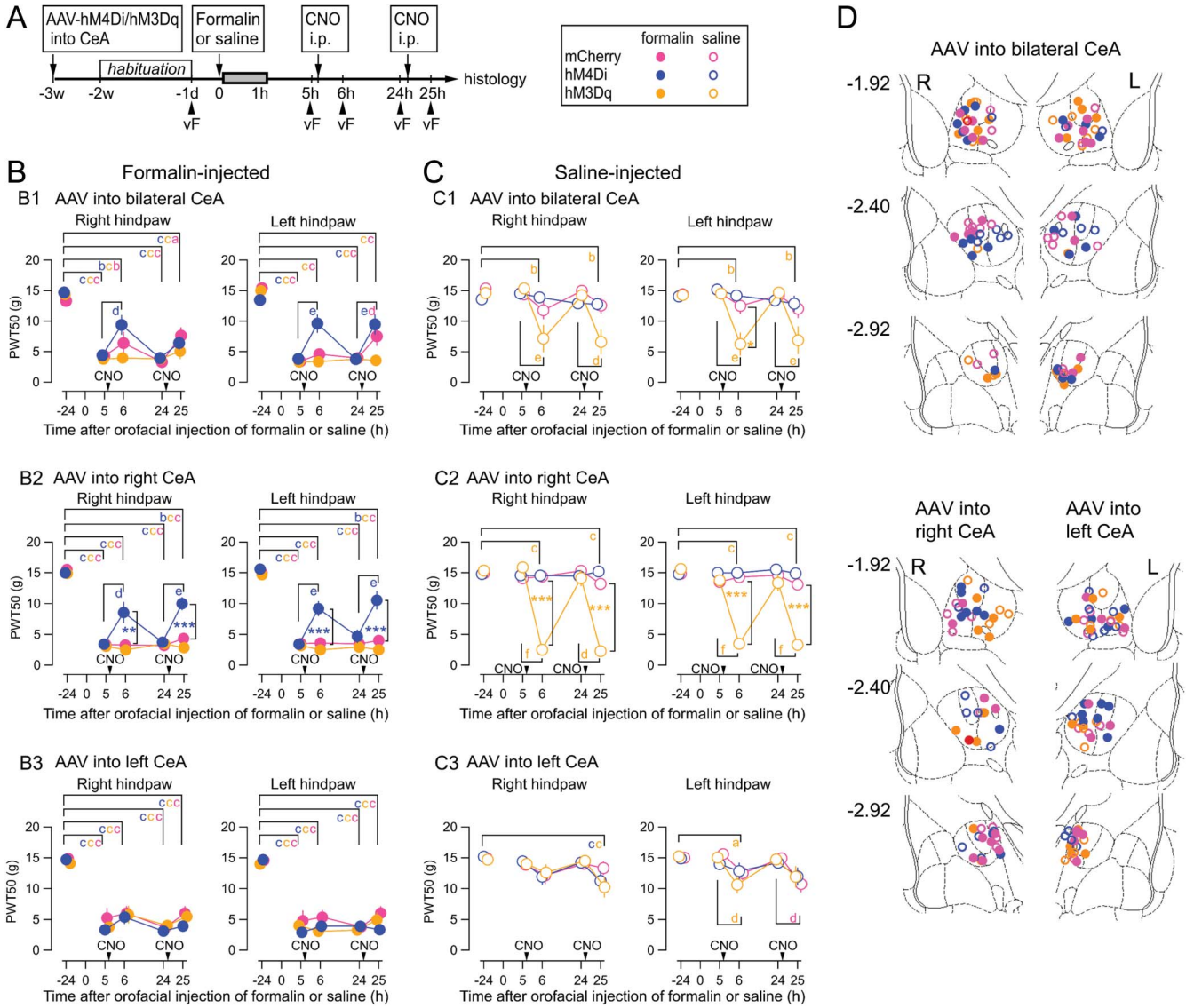

Figure 2. Effect of chemogenetic inhibition and activation of the CeA GABAergic neurons on the mechanical withdrawal threshold of the hind paw. (A) Experimental procedure (experiment 2 and 3). Gray rectangle shows the period of video recording for postexperiment confirmation of nocifensive behaviors. All rats receiving formalin showed typical face rubbing, as shown in Fig. 1. Each rat received intraperitoneal injections of CNO at 5.25 hours and 24.25 hours after formalin or saline injection to the upper lip. (B and C) Summary of mechanical PWT50 in the formalin (B)-injected/saline (C)- injected rats expressing hM4Di-mCherry ("hM4Di" in Fig. 2), hM3Dq-mCherry ("hM3Dq" in Fig. 2), or mCherry ("mCherry" in B) in the bilateral (B1 and C1), right (B2 and C2), or left (B3 and C3) CeA. A legend of markers for B, C, and D is the right of A; magenta, blue, and orange circles indicate mCherry, hM4Di, and hM3Dq, respectively, and filled and open circles indicate formalin-injected/saline-injected rats, respectively. Right and left graphs in each panel are PWT50 seconds for left and right hind paws, respectively. A 2-way repeated measures ANOVA is performed to examine the effect of 2 factors (5 time points and 6 treatment-paw combinations) on PWT50. The differences in PWT50 between each time points were analyzed by the Dunnett test, $^{a}P < 0.05$, $^{b}P < 0.01$, and $^{c}P < 0.001$ for the comparison with baseline, $^{d}P < 0.05$, $^{e}P < 0.01$, and $^{f}P < 0.001$ for the comparison between pre-CNO and post-CNO injection. The colors of alphabet of statistical results indicate to which group the significant difference attribute. The difference in PWT50 between 6 groups at each time point was analyzed by Gabriel's test, $^{**}P < 0.01$, $^{***}P < 0.001$. Orange and blue stars in the graphs indicate the difference of hM3Dq-saline vs mCherry-saline and hM4Di-formalin vs mCherry-formalin, respectively. See Table 1, available at http://links.lww.com/PAIN/B291 for detailed statistical results. The numbers of rats are 10 (hM4Di-formalin), 6 (hM4Di-saline), 8 (hM3Dq-formalin), 7 (hM3Dq-saline), 9 (mCherry-formalin), and 10 (mCherry-saline) for B1 and C1; 9 (hM4Di-formalin), 10 (hM4Di-saline), 10 (hM3Dq-formalin), 6 (hM3Dq-saline), 10 (mCherry-formalin), and 9 (mCherry-saline) for B2 and C2; 11 (hM4Di-formalin), 11 (hM4Di-saline), 10 (hM3Dq-formalin), 11 (hM3Dq-saline), 11 (mCherry-formalin), and 10 (mCherry-saline) for B3 and C3. (D) Histological identification of the injection sites of AAV solutions in the CeA. Each circle indicates the tip of the injection in the diagrams of 3 coronal sections, −1.92 mm, −2.40 mm, and −2.92 mm from the bregma. Magenta-filled circles, mCherry-formalin; magenta-open circles, mCherry-saline; blue-filled circles, hM4Di-formalin; blue-open circles, hM4Di-saline; orange-filled circles, hM3Dq-formalin; orange-open circles, hM3Dq-saline. The distribution of mCherry-expression is shown in Fig. S5 (available at http://links.lww.com/PAIN/B292). CNO, clozapine N-oxide.

right CeA, was occluded by prior inflammatory pain. This result further supports the notion that facial inflammation caused mechanical hypersensitivity in bilateral hind limbs primarily through exciting right CeA neurons.

The results in the rats with formalin injection shown in **Figure 2B** indicate that the right CeA regulates the intensity of mechanosensitivity in remote limbs in the rats with orofacial inflammation. One of the interpretations of this result is that the sustained neuronal activities in the right CeA, resulting from inflammatory inputs through parabrachio–amygdaloid pathways,[56] increase the spinal input gain to mechanosensation, which causes ectopic hypersensitivity. If this is the case, it could

be expected that selective artificial excitation of the CeA neurons would cause mechanical hypersensitivity in the hind limbs.

To directly examine this hypothesis, we compared the effects of CNO in rats expressing hM3Dq, hM4Di, and mCherry after saline injection (**Fig. 2C**). Unlike significant and manifest decrease in PWT50 after facial formalin injection in all groups (**Fig. 2B**), the saline injection did not affect PWT50 regardless of the type and side of AAV transfection (**Fig. 2C**). In the rats without inflammation, an injection of CNO significantly decreased the PWT50 of bilateral hind limbs in rats with hM3Dq expression in the bilateral or right CeA (open orange circles in **Figs. 2C1 and C2**). This significant reduction in the threshold by CNO injection was repeatedly observed at the second injection made at 19 hours after the first injection (orange-open circles at 25 hours in **Figs. 2C1 and C2**). Such reduction in PWT50 in saline-treated rats did not occur in the rats expressing hM4Di or mCherry in the bilateral (**Fig. 2C1**) or right (**Fig. 2C2**) CeA. By contrast, the rats with the left CeA transfection did not show such a marked change in the PWT50 by CNO injection (orange open circles in **Fig. 2C3**). As a whole, these results support the notion that activation of neurons in the right CeA is sufficient to induce mechanical hypersensitivity in the hind limb, even in the absence of facial inflammation.

In this series of experiments shown in **Figure 2**, we used the response to CNO in the rats expressing mCherry in the CeA as the control to the DREADD activation.[53] However, in a part of the experiments, we observed slight but significant changes in PWT50 in rats expressing mCherry (magenta-filled circle in the left hind paw at 25 hours in **Fig. 2B1** and magenta open circle in the left hind paw at 25 hours in **Fig. 2C3**). Although not significantly, CNO markedly shifted PWT50 in the right hind paw at 6 hours in mCherry-expressing formalin-injected rats (magenta-filled circle **Fig. 2B1**). In addition, we occasionally observed unexpected nonsignificant shifts in PWT50 by CNO regardless of the type of AAV vector injected in both formalin-injected and saline-injected groups (eg, **Fig. 2B3**, right hind paw; **Fig. 2C3**, right and left hind paw, at 6 and 25 hours). However, such CNO effects were not consistently observed in other CNO administration cases than listed here. In most cases, changes in PWT50 by CNO were negligibly small and not significant (magenta-filled and open circles in **Figs. 2B and C**; statistical results of Dunnett's test for these nonsignificant cases are shown in Table 1, available at http://links.lww.com/PAIN/B291). One of the possible mechanisms underlying these unexpected effects of CNO would be the "off-target" effects of CNO, which are known to depend on the metabolic rate of CNO to clozapine[54] and the stress state of the animals.[55] The exact reason why such off-target CNO effects were observed in particular experimental cases remains undetermined.

The expression of Venus fluorescence in rats produced by crossing ROSA26/CAG-floxed STOP-ChRFR (C167A)-Venus BAC rat and the same line of VGAT Cre rat as used in this study is limited to GABAergic cells in broad regions of the brain and indeed overlap with GABA immunoreactivity.[36] Soma et al. also confirmed the coexpression of Cre-dependent tdTomato in the same VGAT-cre rats and GABA immunoreactivity in the motor cortex.[78] In this study, we demonstrated that Cre recombinase expression is limited to the GABAergic cells in the amygdala by multiplex fluorescent in situ hybridization. The fluorescent signals for mRNAs of VGAT (light-blue dots in Fig. S3A and its higher-magnitude image of the white-framed square in Fig. S3A and Fig. S3B, available at http://links.lww.com/PAIN/B292) were densely observed in the CeA, as expected, and much sparsely in the BLA, also as expected. A larger-magnitude view of region 1 from the CeA in Figure S3B (the white-framed square numbered "1" in Fig. S3B, available at http://links.lww.com/PAIN/B292) indicates that Cre recombinase mRNA signals (red dots in images in Figs. S3A and S3B, available at http://links.lww.com/PAIN/B292) are colocalized with VGAT mRNA signals (light-blue signals), but never with VGLUT signals (dark-blue signals). Expression of mCherry (red points in Fig. S3C1 and S3C2, available at http://links.lww.com/PAIN/B292), of which the expression was driven by Cre recombinase associated with VGAT expression, was limited to the CeA around the injected fluorescence beads (blue signal in Fig. S3C1 and S3C2, available at http://links.lww.com/PAIN/B292). Such a limited expression of mCherry was observed in a large set of the rats tested. Even in the cases in which we could observe the expression of mCherry in surrounding structures of the CeA, their density was much sparser compared with those within the CeA.

Figure 2D indicates the intra-CeA injection sites as confirmed with the microbeads fluorescence after the behavioral data collection (**Fig. 2**). In the successful experiments, the tip of the pipette (the highest beads density in the slice) was consistently found within the CeA and surrounded by many neurons expressing mCherry (Figure S3C1 and S3C2, available at http://links.lww.com/PAIN/B292). To depict how the expression of transfected genes and their products spread around the injection site, we drew the border of mCherry expression for each slice according to a procedure explained in Figure S4 (available at http://links.lww.com/PAIN/B292), and the transfected regions were collectively presented for all the rats tested in Figure S5 (available at http://links.lww.com/PAIN/B292). In all rats, the mCherry signal covered a large portion of CeA regions in each group, suggesting CNO was expressed in a significant amount of CeA neurons. However, in some rats, an extra-CeA mCherry signal was also observed and not negligible. These signals might represent the expression of cre recombinase in GABAergic neurons outside of the CeA, such as the caudate putamen and basolateral amygdala. They would also contain GABAergic neurons in the adjacent intercalated cell mass, which is difficult to manipulate in isolation because it is too close and small. It remains to be analyzed how inhibition or activation of GABAergic neurons in these extra-CeA regions affects PWT50. Because of the consistent mCherry expression in all rats tested in the CeA and sporadic and additional extra-CeA expressions, it is likely that the consistently observed effects of CNO application primarily resulted from activation of DREADDs mainly in the CeA. As a summary, these results definitively indicate that (1) selective inhibition of the GABAergic neurons in the right CeA attenuates the widespread hypersensitivity in the bilateral hind limbs of rats caused by orofacial inflammatory pain and (2) selective excitation of the GABAergic neurons in the right CeA gives rise to hypersensitivity in the bilateral hind limbs of rats without inflammation and pain.

3.3. Clozapine N-oxide directly affected neuronal excitability of the neurons expressing designer receptor exclusively activated by a designer drug in ex-vivo slices

The DREADDs transfected into the CeA are metabotropic G-protein coupled receptors associated with Gq (hM3Dq) or Gi (hM4Di). As the consequences of activating these receptors depend on the type of downstream enzymatic machinery, it is necessary to confirm the effects of their activation in the cells to be examined. As proof, we confirmed that pharmacological activation of DREADDs with CNO, affects the excitability of the CeA neurons expressing mCherry with DREADDs in the ex-vivo brain slice preparations, which were prepared from a subset of randomly chosen rats at 5 to 8 weeks after AAV injection. In the

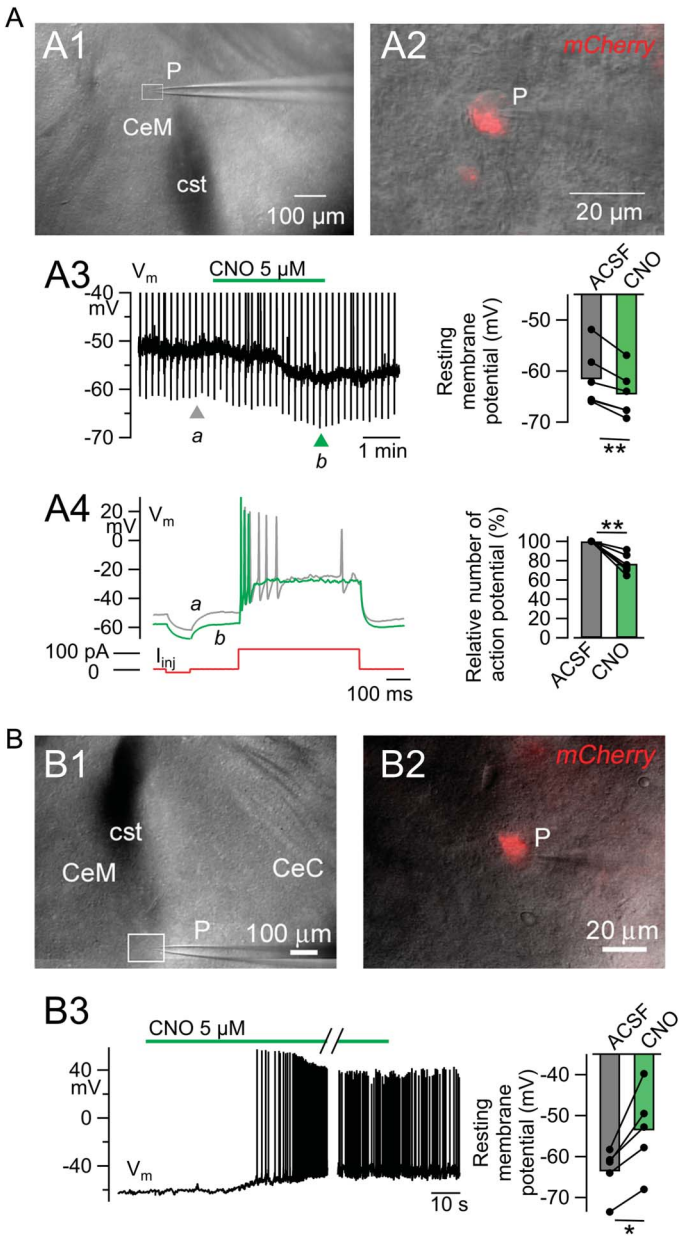

Figure 3. Electrophysiological recording of CNO-induced response from the CeM neurons expressing hM4Di or hM3Dq in acute amygdalar slices. (A) CNO-induced hyperpolarization of membrane potential in the hM4Di-mCherry expressing CeA neurons. A1, Typical example of the coronal slice, including the CeA used for patch-clamp recording. CeM, medial subdivision of the CeA. cst, commissural stria terminalis. P, recording pipette. A2, Magnified image of the area indicated with a rectangle in A1. Whole-cell recordings were performed from hM4Di-mCherry-positive cells. A3, Effect of CNO on the resting membrane potential in hM4Di-mCherry-positive cells. A representative trace of the patch-clamp recording (left) recorded from the hM4Di-mCherry-positive neuron shown in A2 in the current-clamp mode. The regularly repeated vertical shifts represent parts of passive membrane responses to hyperpolarizing and depolarizing currents injected every 10 seconds. A rectangular hyperpolarizing pulse (100-300 ms, −20 pA) followed by a depolarizing pulse (500 ms, 100-120 pA) was injected every 10 seconds, the responses to which are truncated in A3 so that the change in resting membrane potential is more visible. The right panel of A3 shows the summary of the resting membrane potential under the ACSF and during the addition of CNO. CNO (5 μM) hyperpolarized hM4Di-mCherry-positive neurons; $^{**}P < 0.01$, ACSF vs CNO; paired *t* test, n = 6 neurons from 2 rats. A4, the effect of CNO on the response to inward current injection. Current injection generated action potentials. Gray and green traces in A4 left panel were recorded under the normal ACSF before applying CNO at the point of the gray arrowhead (A) in A3 left panel and after applying CNO at the point of the green arrowhead (B) in A3 left panel, respectively. The red line at the bottom of A4 left panel indicates the injected current step. The right panel of A4 shows the summary of the number of action potentials normalized by that under ACSF. CNO (5 μM) hyperpolarized the membrane potential and decreased the number of action potentials in hM4Di-mCherry-positive neurons; $^{**}P < 0.01$, ACSF vs CNO; paired *t* test. (B) CNO-induced depolarization of membrane potential in the hM3Dq-mCherry expressing CeA neurons. B1, Typical example of the coronal slice, including the CeA used for patch-clamp recording. CeM, the medial subdivision of the CeA. CeC, the capsular subdivision of the CeA. cst, commissural stria terminalis. P, recording pipette. B2, Magnified image of the area indicated with a rectangle in B1. Whole-cell recordings were performed from hM3Dq-mCherry-positive cells. B3, Effect of CNO on the resting membrane potential in hM3Dq-mCherry-positive cells. A representative trace of the patch-clamp recording (B3-left) was recorded from the hM3Dq-mCherry-positive neuron shown in B2 in the current-clamp mode. The right panel summarizes the resting membrane potentials under the ACSF (before CNO) and CNO (after CNO). Clozapine N-oxide (5 μM) depolarized hM3Dq-mCherry-positive neurons; $^{*}P < 0.05$, ACSF vs CNO; paired *t* test. The neurons in A expressing hM4Di receptors were recorded from the most lateral portion of the CeM (A1; 2 cells from the left and 4 cells from the right) prepared from 2 rats. The 5 neurons in B expressing hM3Dq receptors were recorded also from the most lateral portion of the CeM (B1; 1 cell from the left and 4 cells from the right) prepared from 3 rats. There was no apparent difference in the membrane properties and responses to CNO depending on the side and location of the cells. ACSF, artificial cerebrospinal fluid; CNO, clozapine N-oxide.

hM4Di-transfected rats (**Figs. 3A1 and A2**), application of CNO (5 μM) significantly hyperpolarized the CeA neurons (**Fig. 3A3**) and decreased the number of action potentials in response to depolarizing pulse in the CeA neurons (**Fig. 3A4**) showing mCherry fluorescence (**Fig. 3A2**). The CeA neurons showing mCherry fluorescence in the rats that received hM3Dq expression vector (**Figs. 3B1 and B2**), were significantly depolarized by CNO (5 μM), accompanied by the generation of action potentials (**Fig. 3B3**). These responses were consistently observed in all the neurons examined. These results indicate that the synthetic ligand CNO directly excites (hM3Dq-expressing) and inhibits (hM4Di-expressing) neurons in the CeA, thus supporting the interpretation that the experimental modulation of the CeA neuron excitability alone is sufficient to modulate nociceptive behaviors.

3.4. Blockade of calcitonin gene–related peptide receptors in the right central amygdala attenuated ectopic sensitization in the rats with orofacial inflammation

The CeA is rich in receptors for CGRP, which are likely to be activated by CGRP released from the axon terminals of LPB origin.[18,46] Exogenous CGRP increases postsynaptic N-methyl-D-aspartate receptor-mediated current at the LPB-CeC synapse,[63] and endogenous CGRP is necessary in the LPB-CeC synaptic potentiation.[75] A very interesting finding by the group of Neugebauer is that blockade of CGRP receptors in the CeA with $CGRP_{8-37}$ can attenuate already established pain sensitization at the knee joint of arthritis rats, indicating that CGRP receptors in the arthritis rats are continuously activated in a manner blocked by a selective antagonist.[35] Furthermore, they demonstrated blockade of CGRP receptors in the brain slice, where there was no more source of CGRP, can cancel the LPB-CeA synaptic potentiation in the slices prepared from arthritis rats.[35] These lines of evidence suggest that the blockade of CGRP receptors in rats with augmented CeA neuron activities resulting from inflammatory pain can attenuate the potentiated nocifensive response at the site of injury/inflammation. Therefore, we examined whether the blockade of the CGRP receptors in the CeA could also affect the ectopic sensitization in the hind limb after orofacial inflammation (**Fig. 4**). **Figure 4A** shows the timings of manipulations. Microinjection of $CGRP_{8-37}$, a partial peptide that selectively blocks CGRP receptors, into bilateral CeAs at a concentration reported to block CGRP receptors,[35] slightly but significantly recovered the bilateral PWT50 lowered after formalin injection to the left upper lip (green-filled circles in **Fig. 4B1**). This effect was repeatedly observed when the CGRP receptor antagonist was injected at 5.5 hours postformalin and almost faded at ~20 hours later. Injection of the CGRP receptor antagonist to the regions outside of the CeA (striatum) did not affect the lowered PWT50 in formalin-injected rats (red-filled circles in **Fig. 4B1**). Again, this attenuation in the formalin-induced hypersensitivity after intra-CeA injection of CGRP receptor antagonist was most prominent when the blocker was injected only to the right CeA (**Fig. 4B2**) but was not observed after the left CeA injection (**Fig. 4B3**). **Figure 4C** indicates the site of injections confirmed after behavior experiments using fluorescent beads injected with the CGRP receptor antagonist solution. Altogether, as with the mechanical sensitization in the knee joint arthritis model,[59] blockade of CGRP receptors in the CeA can significantly attenuate ectopic sensitization in the hind paw in the orofacial inflammatory pain model.

4. Discussion

Here, we presented a novel widespread/ectopic pain model in which mechanical hypersensitivity occurs in body regions remote to the primary inflammation. In this model, the inflammation was located in the orofacial area innervated by the trigeminal nerve, and the mechanical sensitization occurred in the bilateral hind paws innervated by the lumbar spinal nerves. Based on the results of chemogenetics and pharmacological experiments, we conclude that the GABAergic neurons in the right CeA, a site selectively activated by sustained nociceptive/inflammatory inputs by trigeminal afferents,[56] play an essential role in this remote sensitization. The involvement of the left CeA seems limited. The most straightforward interpretation is that the right CeA activated by the nociceptive/inflammatory information in one part of the body augments the sensitivity of the nociceptive responses to mechanical touch in other parts of the body. This amygdala-regulated sensitization could have a protective function in avoiding further injury to the body by raising the level of vigilance to the external environment when an individual already has inflammation/persistent pain in one part of the body.[23]

This result also has a significant implication on the study of pain mechanisms in general. Mechanical sensitization in the hind limbs is a hallmark symptom in various animal models of pain. The von-Frey filament test is a gold standard used in most preclinical studies analyzing the intensity of pain in the hind limb in various models.[6,66] The present results imply that the mechanical sensitization in these models might result, at least in part, from enhanced CeA-mediated regulation caused by sustained nociception/inflammation and may not be a simple consequence of the injury and inflammation at the sites of origin. However, this interpretation might depend on the pain model used. In the spinal nerve injury model of rats, the LPB to CeA synaptic potentiation is injury-side dependent and mechanical allodynia occurs only on the injury side.[37] This side specificity is dependent on the progress of pain behaviors.[30] As a whole, the type of the pain model (eg, with or without inflammation) and progress of the nociplastic process would largely affect the occurrence of this amygdala-driven widespread sensitization. This conclusion would have a significant implication for interpreting the lowered mechanical threshold in the hind paw in many "pain-resembling" animal models. Similar remote sensitization has been described in patients with temporomandibular disorders,[16,31,73] migraine,[7,10,14] and knee osteoarthritis.[5,24] As feeling "pain" in a body part where there is no clear sign of injury/inflammation is a perplexing and devastating experience, understanding the mechanism underlying widespread pain and the role played by the CeA is an urgent issue to be examined using brain imaging.[28]

4.1. The amygdala as a site of convergence and divergence with limited somatotopy

The CeA is strategically well situated for a kernel site for widespread hypersensitivity. First, the CeA neurons are activated by sensory information with only limited somatotopic specificity,[61] indicating that nociceptive/inflammatory information arising from widespread body regions converges to the CeA, particularly to the right CeA, while losing the precise information on the site of origin.[56] In rats, the receptive field of the right CeA neurons covers multiple regions of the body and becomes entirely widespread at 2 to 6 hours after left-knee induction of arthritis.[61] Altogether, it is likely that pain-associated sensory inputs activate CeA neurons with a limited somatotopic specification of the origin.

Second, artificial or pharmacological activation of the CeA neurons alone sensitizes the peripheral nociceptive responses in various parts of the body. For example, the pharmacological activation of mitogen-activated protein kinase in the CeA alone lowers the mechanical allodynia threshold in the hind paw.[17] As a

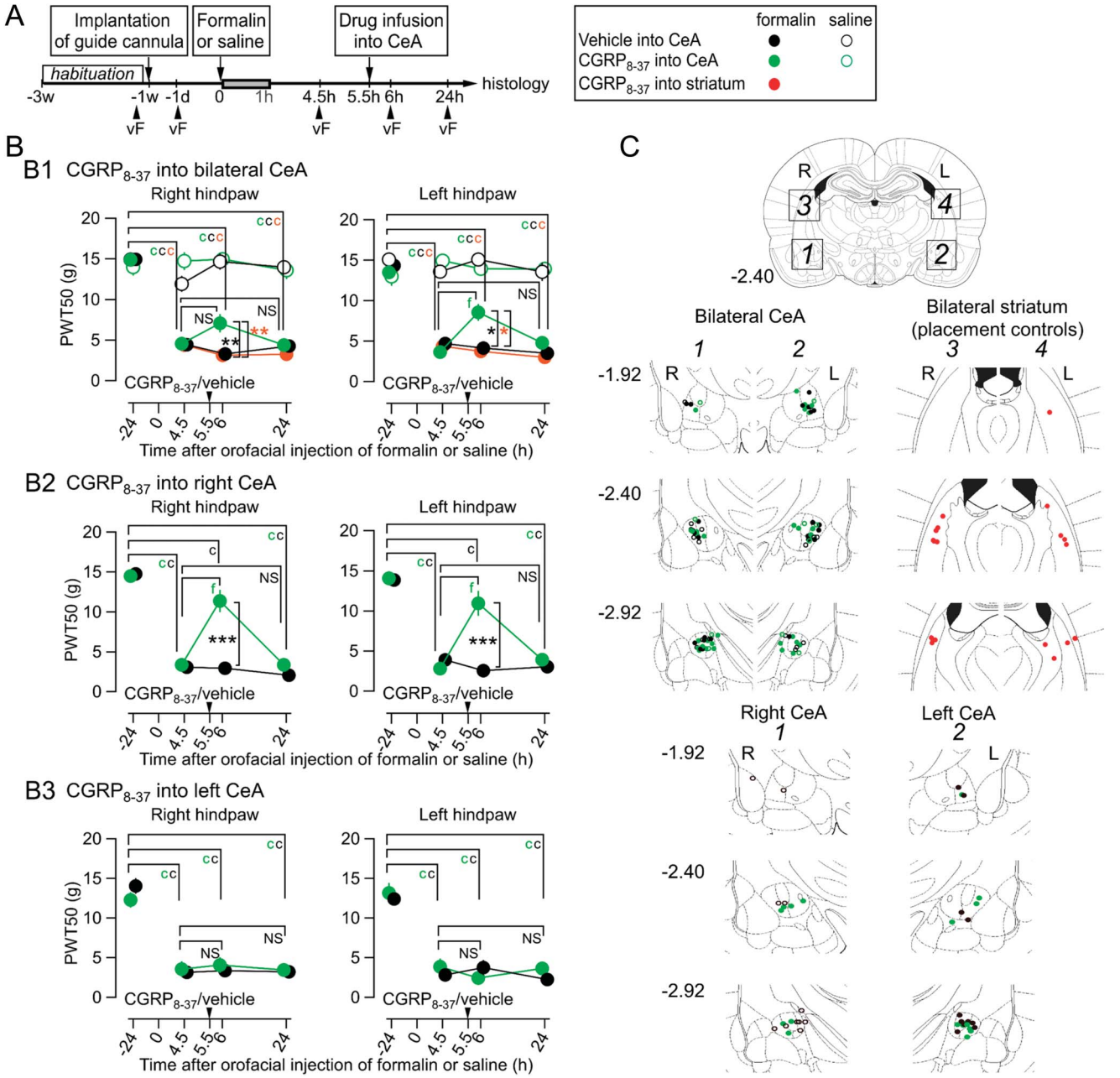

Figure 4. Effects of CGRP receptor antagonist microinjection in the CeA on the mechanical withdrawal threshold of the hind paws in rats with an upper lip formalin or saline injection. (A) Experimental procedure (experiment 4). The pharmacological blockade of the CGRP receptors in the CeA was performed 5.5 hours after formalin/saline injection. (B) CGRP receptor antagonizing peptide, $CGRP_{8-37}$ was infused in the bilateral (B1), right (B2), or left CeA (B3). A legend of markers for B and C is shown at the right of A; black, green, and red circles indicate the group of the vehicle into the CeA, $CGRP_{8-37}$ into the CeA, and $CGRP_{8-37}$ into the striatum, respectively, and filled and open circles indicate formalin-injected/saline-injected rats, respectively. A 2-way repeated-measures ANOVA is performed to examine the effect of 2 factors (4-time points and 2 or 5 treatment groups) on the PWT50. The difference in PWT50 between each time point was analyzed by Dunnett test, $^{c}P < 0.001$ for the comparison with baseline, $^{f}P < 0.001$ for the comparison between pre- $CGRP_{8-37}$ and post-$CGRP_{8-37}$ injection. The colors of the alphabet of statistical results indicate to which group the significant difference attribute. In the formalin group, $CGRP_{8-37}$ into bilateral (B1) or right (B2) CeA significantly raised the lowered PWT50 transiently, which decreased again at 24 hours ($^{f}P < 0.001$, Dunnett test; 4.5 hours vs 6 hours postformalin). This was not the case in rats with vehicle injection and with striatum injection of $CGRP_{8-37}$. The differences in PWT50 between groups at each time point was analyzed by Gabriel's test ($^{*}P < 0.05$, $^{**}P < 0.01$, formalin-$CGRP_{8-37}$ vs formalin-vehicle (black stars) and $^{***}P < 0.001$, formalin-$CGRP_{8-37}$ vs formalin-striatum (orange stars) for B1) or Mann–Whitney *U* test ($^{***}P < 0.001$, formalin-$CGRP_{8-37}$ vs formalin-vehicle (black stars) for B2). There was no significant difference between groups in B3 (refer to Table 1, available at http://links.lww.com/PAIN/B291). The numbers of rats are 15 ($CGRP_{8-37}$-formalin), 8 ($CGRP_{8-37}$-saline), 10 ($CGRP_{8-37}$ into striatum-formalin), 12 (vehicle-formalin), 9 (vehicle-saline) for B1; 7 ($CGRP_{8-37}$-formalin), 11 (vehicle-formalin) for B2; 9 ($CGRP_{8-37}$-formalin), 8 (vehicle-formalin) for B3. (C) Histological identification of the local infusion sites of $CGRP_{8-37}$. The scheme at the top of Fig. 4C indicates the target area of microinjection. Squares no. 1 and 2 show the regions containing the amygdala, and squares no. 3 and 4, show the striatum. Bottom panels show the sites of injection cannula-tip plotted in the 3 coronal sections, −1.92, −2.40, and −2.92 from the bregma, adapted from the atlas by Paxinos and Watson (2007), in each experimental group. The color indicates each group (see the legend in the box at the right top of Fig. 4). The distribution of FluoSphere is shown in Fig. S6 (available at http://links.lww.com/PAIN/B292). ANOVA, analysis of variance; CGRP, calcitonin gene–related peptide.

sequel to this pioneering work, it has been shown that chemogenetic activation of protein kinase C δ-expressing right CeA neurons caused mechanical as well as thermal (hot and cold) allodynia in bilateral hind paws.[85] Pharmacological activation of CGRP1 receptors, metabotropic glutamate receptor 5 (mGluR5), and corticotropin-releasing factor receptor type-1 receptors in the CeA and an injection of reactive oxygen species scavenger into the right CeA sensitizes the knee joint to mechanical stimulation[34,35,39,40,60] or visceral nocifensive movements.[22,41,42,57,67] Such influence from the CeA to widespread regions might provide a basis for widespread pain in primary chronic pain, which occurs even in the absence of injury or inflammation. Combining these 2 aspects, that is, the convergence and divergence of the pain-associated inputs and outputs to/from the CeA, it is likely that the CeA plays a "hub" role through being activated by the diverse regions of the body, which in turn modulates the nociceptive sensitivity in widespread regions, as observed in this study.

4.2. The remaining issues found in this study and to be answered in the future studies

Four other issues should be addressed to extend the present results.

4.2.1. How does the modulation of the CeA network affect nocifensive sensitivity?

The CeA neurons, that is, the capsular (CeC), lateral (CeL), and medial (CeM) CeA neurons,[64] are mostly GABAergic.[47,83] In addition, the outputs from the CeA network, mostly originated in the CeM and partly in the CeL, are also GABAergic. This anatomo-functional situation makes it extremely difficult to understand how an experimental manipulation of an CeA network element alters the CeA-regulated nocifensive behaviors. It remains unclear how excitation and inhibition of the GABAergic neurons in the CeC, CeL, and CeM modulate allodynia. It is most likely that the direct suppression or excitation of the CeM neurons transmit final outputs to the modules for descending pain modulation, such as the ventrolateral periaqueductal grey,[50] by DREADDs would be most influential in affecting pain-like behaviors. The roles played by the CeM neurons in the nociceptive behavior regulation remain to be identified in future studies.[50]

4.2.2. Laterality

Similar to the right side predominant activation of the CeA after formalin injection,[56] the present results indicate that the right CeA also plays the predominant role in regulating mechanical sensitivity. Such laterality in the CeA function in pain models is a hot topic.[3] We failed to observe major significant changes in the PWT50 by modulating left CeA activity alone, unlike the abdominal nocifensive behavior in the bladder-stimulated rats.[72] However, the effects of bilateral modulation were less manifest (ie, changes, if any, were less supported by statistical significance) than those of right-CeA-only modulation. Thus, it is suggested that the left CeA activity would also play any role, which is rather analgesic, in regulating touch-induced escape behavior. It is also possible that the antinociceptive role of the left CeA would require other evaluation of a different kind of pain than the von Frey test. At this moment, the mechanism underlying this right-side predominance of the CeA in the regulation of mechanical sensitivity remains undetermined and needs to be determined in future studies.

4.2.3. The sex of the experimental animals

In this study, we used male rats. The sex-dependent difference in the mechanism underlying sustained pain in animals has been repeatedly shown and acknowledged to be one of the most influential factors of pain behaviors.[77] It is an exciting future question to be addressed whether the effects of chemogenetic manipulation of the CeA on mechanical sensitivity is also observed in female animals. This is a testable question and should be asked in the near future.

4.2.4. Technical limitations with chemogenetics experiments

In this study, we used CNO, a most conventionally used ligand, to activate DREADDs. Clozapine N-oxide is readily metabolized to clozapine, which can activate a wide range of endogenous receptors,[29] suggesting that the observed effects might have involved a synergic activation of DREADDs and other targets outside of the CeA. Use of recently developed more selective ligand[58] and more targeted expression system, such as those with FosTRAP mice[32] would allow gaining more detailed scenario as to how CeA neurons regulate widespread peripheral sensitivity.

4.3. Functional implications

In the latest edition of the International Classification of the Diseases-11 by the World Health Organization (2018), "chronic widespread pain (MG30.01)" is a subclass of the primary chronic pain defined as "diffuse pain in at least 4 of 5 body regions and is associated with significant emotional distress or functional disability." Fibromyalgia is included in this class. Brain imaging studies in human fibromyalgia patients demonstrated aberrant morphological and functional alteration in the amygdala.[12,28,38,43] As the amygdala, particularly the CeA, is a hub site for emotional responses and a central target for stress-associated or inflammation-associated mediators, in addition to nociception, we predict here that the CeA would be the kernel site that underlies widespread pain, such as in fibromyalgia.

5. Conclusions

Plastic ("nociplastic") changes would be the hallmark of the amygdala network function to the convergence of nociceptive signals and divergence of nocifensive behavior-associated command to the whole body. This mechanism should have evolutional significance by elevating the vigilance level in response to ongoing injury/inflammation to protect against the further risk to survival.[23,52]

Conflict of interest statement

The authors have no conflicts of interest to declare.

Acknowledgments

This study was supported in part by JSPS KAKENHI Grants to F. Kato (19H04759 and 18H02722), to Y.K. Sugimura (19K16932), and Y. Takahashi (17K09042 and 20K09207) and MEXT-Supported Program for the Strategic Research Foundation at Private Universities, S1311009 (2013-2019). This was work was also supported by the Uehara Memorial Foundation and the Naito Foundation. The W-Tg(Slc32a1-cre)$^{3\_5Fusa}$ rat was developed by authors with support from the C.B.S.N project conducted by Drs.

K. Kobayashi (Fukushima Medical University) and Y. Yanagawa (Gumma University), using a VGAT-cre BAC construct developed by Dr. S. Itohara (RIKEN). Contribution of Ms. Hazuki Sato (Laboratory Animal Facility, Jikei University School of Medicine) to the establishment of this transgenic rat is acknowledged. The authors have no conflicts of interest in relation to the contents of this article.

Appendix A. Supplemental digital content

Supplemental digital content associated with this article can be found online at http://links.lww.com/PAIN/B291 and http://links.lww.com/PAIN/B292.

Article history:
Received 21 August 2020
Received in revised form 1 January 2021
Accepted 26 January 2021

References

[1] Aicher SA, Hegarty DM, Hermes SM. Corneal pain activates a trigemino-parabrachial pathway in rats. Brain Res 2014;1550:18–26.
[2] Aicher SA, Hermes SM, Hegarty DM. Corneal afferents differentially target thalamic- and parabrachial-projecting neurons in spinal trigeminal nucleus caudalis. Neuroscience 2013;232:182–93.
[3] Allen HN, Bobnar HJ, Kolber BJ. Left and right hemispheric lateralization of the amygdala in pain. Prog Neurobiol 2020;196:101891. doi:10.1016/j.pneurobio.2020.101891.
[4] Ambriz-Tututi M, Rocha-González HI, Castañeda-Corral G, Araiza-Saldaña CI, Caram-Salas NL, Cruz SL, Granados-Soto V. Role of opioid receptors in the reduction of formalin-induced secondary allodynia and hyperalgesia in rats. Eur J Pharmacol 2009;619:25–32.
[5] Arendt-Nielsen L, Nie H, Laursen MB, Laursen BS, Madeleine P, Simonsen OH, Graven-Nielsen T. Sensitization in patients with painful knee osteoarthritis. PAIN 2010;149:573–81.
[6] Barrot M. Tests and models of nociception and pain in rodents. Neuroscience 2012;211:39–50.
[7] Bernstein C, Burstein R. Sensitization of the trigeminovascular pathway: perspective and implications to migraine pathophysiology. J Clin Neurol 2012;8:89.
[8] Bianchi M, Martucci C, Biella G, Ferrario P, Sacerdote P. Increased substance P and tumor necrosis factor-α level in the paws following formalin injection in rat tail. Brain Res 2004;1019:255–8.
[9] Bianchi M, Panerai AE. Formalin injection in the tail facilitates hindpaw withdrawal reflexes induced by thermal stimulation in the rat: effect of paracetamol. Neurosci Lett 1997;237:89–92.
[10] Bigal ME, Ashina S, Burstein R, Reed ML, Buse D, Serrano D, Lipton RB. Prevalence and characteristics of allodynia in headache sufferers: a population study. Neurology 2008;70:1525–33.
[11] Boyer N, Dallel R, Artola A, Monconduit L. General trigeminospinal central sensitization and impaired descending pain inhibitory controls contribute to migraine progression. PAIN 2014;155:1196–205.
[12] Burgmer M, Gaubitz M, Konrad C, Wrenger M, Hilgart S, Heuft G, Pfleiderer B. Decreased gray matter volumes in the cingulo-frontal cortex and the amygdala in patients with fibromyalgia. Psychosom Med 2009;71:566–73.
[13] Burgos-Vega CC, Ahn DDU, Bischoff C, Wang W, Horne D, Wang J, Gavva N, Dussor G. Meningeal transient receptor potential channel M8 activation causes cutaneous facial and hindpaw allodynia in a preclinical rodent model of headache. Cephalalgia 2016;36:185–93.
[14] Burstein R, Yarnitsky D, Goor-Aryeh I, Ransil BJ, Bajwa ZH. An association between migraine and cutaneous allodynia. Ann Neurol 2000;47:614–24.
[15] Cadet R, Aigouy L, Woda A. Sustained hyperalgesia can be induced in the rat by a single formalin injection and depends on the initial nociceptive inputs. Neurosci Lett 1993;156:43–6.
[16] Campi LB, Jordani PC, Tenan HL, Camparis CM, Gonçalves DAG. Painful temporomandibular disorders and central sensitization: implications for management—a pilot study. Int J Oral Maxillofac Surg 2017;46:104–10.
[17] Carrasquillo Y, Gereau RW. Activation of the extracellular signal-regulated kinase in the amygdala modulates pain perception. J Neurosci 2007;27:1543–51.
[18] Carter ME, Han S, Palmiter RD. Parabrachial calcitonin gene-related peptide neurons mediate conditioned taste aversion. J Neurosci 2015;35:4582–6.
[19] Chaplan SR, Bach FW, Pogrel JW, Chung JM, Yaksh TL. Quantitative assessment of tactile allodynia in the rat paw. J Neurosci Methods 1994;53:55–63.
[20] Clavelou P, Dallel R, Orliaguet T, Woda A, Raboisson P. The orofacial formalin test in rats: effects of different formalin concentrations. PAIN 1995;62:295–301.
[21] Clavelou P, Pajot J, Dallel R, Raboisson P. Application of the formalin test to the study of orofacial pain in the rat. Neurosci Lett 1989;103:349–53.
[22] Crock LW, Kolber BJ, Morgan CD, Sadler KE, Vogt SK, Bruchas MR, Gereau RW. Central amygdala metabotropic glutamate receptor 5 in the modulation of visceral pain. J Neurosci 2012;32:14217–26.
[23] Crook RJ, Dickson K, Hanlon RT, Walters ET. Nociceptive sensitization reduces predation risk. Curr Biol 2014;24:1121–5.
[24] Fingleton C, Smart K, Moloney N, Fullen BM, Doody C. Pain sensitization in people with knee osteoarthritis: a systematic review and meta-analysis. Osteoarthr Cartil 2015;23:1043–56.
[25] Fu K-Y, Light AR, Maixner W. Long-lasting inflammation and long-term hyperalgesia after subcutaneous formalin injection into the rat hindpaw. J Pain 2001;2:2–11.
[26] Fu K-Y, Light AR, Maixner W. Relationship between nociceptor activity, peripheral edema, spinal microglial activation and long-term hyperalgesia induced by formalin. Neuroscience 2000;101:1127–35.
[27] Fu K-Y, Light AR, Matsushima GK, Maixner W. Microglial reactions after subcutaneous formalin injection into the rat hind paw. Brain Res 1999;825:59–67.
[28] Geuter S, Reynolds Losin EA, Roy M, Atlas LY, Schmidt L, Krishnan A, Koban L, Wager TD, Lindquist MA. Multiple brain networks mediating stimulus–pain relationships in humans. Cereb Cortex 2020;30:4204–19.
[29] Gomez JL, Bonaventura J, Lesniak W, Mathews WB, Sysa-Shah P, Rodriguez LA, Ellis RJ, Richie CT, Harvey BK, Dannals RF, Pomper MG, Bonci A, Michaelides M. Chemogenetics revealed: DREADD occupancy and activation via converted clozapine. Science 2017;357:503–7.
[30] Gonçalves L, Dickenson AH. Asymmetric time-dependent activation of right central amygdala neurones in rats with peripheral neuropathy and pregabalin modulation. Eur J Neurosci 2012;36:3204–13.
[31] Greenspan JD, Slade GD, Bair E, Dubner R, Fillingim RB, Ohrbach R, Knott C, Diatchenko L, Liu Q, Maixner W. Pain sensitivity and autonomic factors associated with development of TMD: the OPPERA prospective cohort study. J Pain 2013;14:T63–74.e6.
[32] Guenthner CJ, Miyamichi K, Yang HH, Heller HC, Luo L. Permanent genetic access to transiently active neurons via TRAP: targeted recombination in active populations. Neuron 2013;78:773–84.
[33] Guettier J-M, Gautam D, Scarselli M, de Azua IR, Li JH, Rosemond E, Ma X, Gonzalez FJ, Armbruster BN, Lu H, Roth BL, Wess J. A chemical-genetic approach to study G protein regulation of cell function in vivo. Proc Natl Acad Sci 2009;106:19197–202.
[34] Han JS, Adwanikar H, Li Z, Ji G, Neugebauer V. Facilitation of synaptic transmission and pain responses by CGRP in the amygdala of normal rats. Mol Pain 2010;6:10.
[35] Han JS, Li W, Neugebauer V. Critical role of calcitonin gene-related peptide 1 receptors in the amygdala in synaptic plasticity and pain behavior. J Neurosci 2005;25:10717–28.
[36] Igarashi H, Ikeda K, Onimaru H, Kaneko R, Koizumi K, Beppu K, Nishizawa K, Takahashi Y, Kato F, Matsui K, Kobayashi K, Yanagawa Y, Muramatsu S-I, Ishizuka T, Yawo H. Targeted expression of step-function opsins in transgenic rats for optogenetic studies. Sci Rep 2018;8:5435.
[37] Ikeda R, Takahashi Y, Inoue K, Kato F. NMDA receptor-independent synaptic plasticity in the central amygdala in the rat model of neuropathic pain. PAIN 2007;127:161–72.
[38] Jensen KB, Loitoile R, Kosek E, Petzke F, Carville S, Fransson P, Marcus H, Williams SCR, Choy E, Mainguy Y, Vitton O, Gracely RH, Gollub R, Ingvar M, Kong J. Patients with fibromyalgia display less functional connectivity in the brain's pain inhibitory network. Mol Pain 2012;8:1744–8069–8:32.
[39] Ji G, Neugebauer V. Pro- and anti-nociceptive effects of corticotropin-releasing factor (CRF) in central amygdala neurons are mediated through different receptors. J Neurophysiol 2008;99:1201–12.
[40] Ji G, Neugebauer V. Reactive oxygen species are involved in group I mGluR-mediated facilitation of nociceptive processing in amygdala neurons. J Neurophysiol 2010;104:218–29.
[41] Johnson AC, Tran L, Greenwood-Van Meerveld B. Knockdown of corticotropin-releasing factor in the central amygdala reverses persistent viscerosomatic hyperalgesia. Transl Psychiatry 2015;5:e517.
[42] Johnson AC, Tran L, Schulkin J, Meerveld BG-V. Importance of stress receptor-mediated mechanisms in the amygdala on visceral pain

perception in an intrinsically anxious rat. Neurogastroenterol Motil 2012; 24:479–86.
[43] Jorge LL, Amaro E. Brain imaging in fibromyalgia. Curr Pain Headache Rep 2012;16:388–98.
[44] Kanda Y. Investigation of the freely available easy-to-use software "EZR" for medical statistics. Bone Marrow Transpl 2013;48:452–8.
[45] Kato F, Sugimura YK, Takahashi Y. Pain-associated neural plasticity in the parabrachial to central amygdala circuit. Adv Exp Med Biol 2018; 1099:157–66.
[46] Kawai Y, Takami K, Shiosaka S, Emson PC, Hillyard CJ, Girgis S, MacIntyre I, Tohyama M. Topographic localization of calcitonin gene-related peptide in the rat brain: an immunohistochemical analysis. Neuroscience 1985;15:747–63.
[47] Kim J, Zhang X, Muralidhar S, LeBlanc SA, Tonegawa S. Basolateral to central amygdala neural circuits for appetitive behaviors. Neuron 2017; 93:1464–79.e5.
[48] Kocorowski LH, Helmstetter FJ. Calcitonin gene-related peptide released within the amygdala is involved in Pavlovian auditory fear conditioning. Neurobiol Learn Mem 2001;75:149–63.
[49] Kopruszinski CM, Navratilova E, Swiokla J, Dodick DW, Chessell IP, Porreca F. A novel, injury-free rodent model of vulnerability for assessment of acute and preventive therapies reveals temporal contributions of CGRP-receptor activation in migraine-like pain. Cephalalgia 2020:033310242095979. doi: 10.1177/0333102420959794.
[50] Li J, Sheets PL. The central amygdala to periaqueductal gray pathway comprises intrinsically distinct neurons differentially affected in a model of inflammatory pain. J Physiol 2018;596:6289–305.
[51] Li K, Lin T, Cao Y, Light AR, Fu K-Y. Peripheral formalin injury induces 2 stages of microglial activation in the spinal cord. J Pain 2010;11:1056–65.
[52] Lister KC, Bouchard SM, Markova T, Aternali A, Denecli P, Pimentel SD, Majeed M, Austin J-S, de C, Williams AC, Mogil JS. Chronic pain produces hypervigilance to predator odor in mice. Curr Biol 2020;30: R866–7.
[53] Mahler SV, Aston-Jones G. CNO evil? considerations for the use of DREADDs in behavioral neuroscience. Neuropsychopharmacology 2018;43:934–6.
[54] Manvich DF, Webster KA, Foster SL, Farrell MS, Ritchie JC, Porter JH, Weinshenker D. The DREADD agonist clozapine N-oxide (CNO) is reverse-metabolized to clozapine and produces clozapine-like interoceptive stimulus effects in rats and mice. Sci Rep 2018;8:3840.
[55] Martinez VK, Saldana-Morales F, Sun JJ, Zhu PJ, Costa-Mattioli M, Ray RS. Off-target effects of clozapine-N-oxide on the chemosensory reflex are masked by high stress levels. Front Physiol 2019;10:512. doi: 10.3389/fphys.2019.00521.
[56] Miyazawa Y, Takahashi Y, Watabe AM, Kato F. Predominant synaptic potentiation and activation in the right central amygdala are independent of bilateral parabrachial activation in the hemilateral trigeminal inflammatory pain model of rats. Mol Pain 2018;14:174480691880710.
[57] Myers B, Greenwood-Van Meerveld B. Divergent effects of amygdala glucocorticoid and mineralocorticoid receptors in the regulation of visceral and somatic pain. Am J Physiol Liver Physiol 2010;298:G295–303.
[58] Nagai Y, Miyakawa N, Takuwa H, Hori Y, Oyama K, Ji B, Takahashi M, Huang XP, Slocum ST, DiBerto JF, Xiong Y, Urushihata T, Hirabayashi T, Fujimoto A, Mimura K, English JG, Liu J, Inoue Kichi, Kumata K, Seki C, Ono M, Shimojo M, Zhang MR, Tomita Y, Nakahara J, Suhara T, Takada M, Higuchi M, Jin J, Roth BL, Minamimoto T. Deschloroclozapine, a potent and selective chemogenetic actuator enables rapid neuronal and behavioral modulations in mice and monkeys. Nat Neurosci 2020;23:1157–67.
[59] Neugebauer V. Amygdala pain mechanisms. Handbook Exp Pharmacol 2015;227:261–84.
[60] Neugebauer V. Metabotropic glutamate receptors—important modulators of nociception and pain behavior. PAIN 2002;98:1–8.
[61] Neugebauer V, Li W. Differential sensitization of amygdala neurons to afferent inputs in a model of arthritic pain. J Neurophysiol 2003;89: 716–27.
[62] Okamoto K, Kimura A, Donishi T, Imbe H, Goda K, Kawanishi K, Tamai Y, Senba E. Persistent monoarthritis of the temporomandibular joint region enhances nocifensive behavior and lumbar spinal Fos expression after noxious stimulation to the hindpaw in rats. Exp Brain Res 2006;170: 358–67.
[63] Okutsu Y, Takahashi Y, Nagase M, Shinohara K, Ikeda R, Kato F. Potentiation of NMDA receptor-mediated synaptic transmission at the parabrachial-central amygdala synapses by CGRP in mice. Mol Pain 2017;13:174480691770920.
[64] Paxinos G, Watson C. The Rat Brain in Stereotaxic Coordinates. 6th ed. Amsterdam: Elsevier, 2007.
[65] Peng K-P, May A. Migraine understood as a sensory threshold disease. PAIN 2019;160:1494–501.
[66] Percie du Sert N, Rice ASC. Improving the translation of analgesic drugs to the clinic: animal models of neuropathic pain. Br J Pharmacol 2014; 171:2951–63.
[67] Prusator DK, Greenwood-Van Meerveld B. Amygdala-mediated mechanisms regulate visceral hypersensitivity in adult females following early life stress. PAIN 2017;158:296–305.
[68] Raboisson P, Dallel R. The orofacial formalin test. Neurosci Biobehav Rev 2004;28:219–26.
[69] Rodriguez E, Sakurai K, Xu J, Chen Y, Toda K, Zhao S, Han BX, Ryu D, Yin H, Liedtke W, Wang F. A craniofacial-specific monosynaptic circuit enables heightened affective pain. Nat Neurosci 2017;20:1734–43.
[70] Roelofs TJM, Verharen JPH, van Tilborg GAF, Boekhoudt L, van der Toorn A, de Jong JW, Luijendijk MCM, Otte WM, Adan RAH, Dijkhuizen RM. A novel approach to map induced activation of neuronal networks using chemogenetics and functional neuroimaging in rats: a proof-of-concept study on the mesocorticolimbic system. Neuroimage 2017;156: 109–18.
[71] Rogan SC, Roth BL. Remote control of neuronal signaling. Pharmacol Rev 2011;63:291–315.
[72] Sadler KE, McQuaid NA, Cox AC, Behun MN, Trouten AM, Kolber BJ. Divergent functions of the left and right central amygdala in visceral nociception. PAIN 2017;158:747–59.
[73] Sarlani E, Greenspan JD. Evidence for generalized hyperalgesia in temporomandibular disorders patients. PAIN 2003;102:221–6.
[74] Sato M, Ito M, Nagase M, Sugimura YK, Takahashi Y, Watabe AM, Kato F. The lateral parabrachial nucleus is actively involved in the acquisition of fear memory in mice. Mol Brain 2015;8:22.
[75] Shinohara K, Watabe AM, Nagase M, Okutsu Y, Takahashi Y, Kurihara H, Kato F. Essential role of endogenous calcitonin gene-related peptide in pain-associated plasticity in the central amygdala. Eur J Neurosci 2017; 46:2149–60.
[76] Sink KS, Davis M, Walker DL. CGRP antagonist infused into the bed nucleus of the stria terminalis impairs the acquisition and expression of context but not discretely cued fear. Learn Mem 2013;20:730–9.
[77] Smith JC. A review of strain and sex differences in response to pain and analgesia in mice. Comp Med 2019;69:490–500.
[78] Soma S, Yoshida J, Kato S, Takahashi Y, Nonomura S, Sugimura YK, Ríos A, Kawabata M, Kobayashi K, Kato F, Sakai Y, Isomura Y. Ipsilateral-dominant control of limb movements in rodent posterior parietal cortex. J Neurosci 2019;39:485–502.
[79] Sugimura YK, Takahashi Y, Watabe AM, Kato F. Synaptic and network consequences of monosynaptic nociceptive inputs of parabrachial nucleus origin in the central amygdala. J Neurophysiol 2016;115: 2721–39.
[80] Todd AJ. Neuronal circuitry for pain processing in the dorsal horn. Nat Rev Neurosci 2010;11:823–36.
[81] Uddin O, Studlack P, Akintola T, Raver C, Castro A, Masri R, Keller A. Amplified parabrachial nucleus activity in a rat model of trigeminal neuropathic pain. Neurobiol Pain 2018;3:22–30.
[82] Vanini G. Sleep deprivation and recovery sleep rrior to a noxious inflammatory insult influence characteristics and duration of pain. Sleep 2016;39:133–42.
[83] Veinante P, Yalcin I, Barrot M. The amygdala between sensation and affect: a role in pain. J Mol Psychiatry 2013;1:9.
[84] Vierck CJ, Yezierski RP, Light AR. Long-lasting hyperalgesia and sympathetic dysregulation after formalin injection into the rat hind paw. Neuroscience 2008;153:501–6.
[85] Wilson TD, Valdivia S, Khan A, Ahn H-S, Adke AP, Martinez Gonzalez S, Sugimura YK, Carrasquillo Y. Dual and opposing functions of the central amygdala in the modulation of pain. Cell Rep 2019;29:332–46.e5.
[86] Wu Y, Willcockson HH, Maixner W, Light AR. Suramin inhibits spinal cord microglia activation and long-term hyperalgesia induced by formalin injection. J Pain 2004;5:48–55.
[87] Xu W, Lundeberg T, Wang Y, Li Y, Yu L-C. Antinociceptive effect of calcitonin gene-related peptide in the central nucleus of amygdala: activating opioid receptors through amygdala–periaqueductal gray pathway. Neuroscience 2003;118:1015–22.
[88] Zhang S-H, Yu J, Lou G-D, Tang Y-Y, Wang R-R, Hou W-W, Chen Z. Widespread pain sensitization after partial infraorbital nerve transection in MRL/MPJ mice. PAIN 2016;157:740–9.